

Linear and Nonlinear Stabilizing Control of Quadrotor UAV

Osama E. Mahmoud, Magdy R. Roman ,John F. Nasry
Mechanical power dept., faculty of engineering - mataria
Helwan University
Cairo, Egypt
Osama_ismail@m-eng.helwan.edu.eg

Abstract— Quadrotor Unmanned Aerial Vehicles (UAVs) are commonly used for complex tasks such as, surveillance, search and rescue in hazard locations for its small size, lightness and robustness. However, the stability of UAVs represents a big challenge due to its high Nonlinear, multivariable, strongly coupled nature. The present work investigates two commonly-used control strategies namely, PD-control with low pass filter and Nonlinear feedback linearization control. The parameters of each controller are optimized to set the time-domain performance within specific constrains. The performances of the two control strategies are simulated and the results are validated on real experiments. The results indicate that Nonlinear control can substantially expand the region of controllable flight angles compared to linear control. It can stabilize the quadrotor system in case of multi angle disturbances. PD-controller with low passes filter shows poor performance when it synchronously controls more than one angle at the same time.

Keywords— Nonlinear Control, PD classical control, Optimization, Feedback-Linearization.

I. INTRODUCTION

Nowadays Unmanned Aerial Vehicles (UAVs) represent an interested research area because of its wide applications such as, military operations (e.g. Border security, correction of coordinates and photography), public application (e.g. Search, rescue, security of petrol pipeline and forest fire) and civilian application (e.g. Shooting movie and analysis of fire gas). UAVs were first introduced in military applications in large sizes and cost. Recently, researchers focused on Micro-UAVs, which appeared as a result of modern mechatronics and microelectronics for the purpose of control algorithm testing and development. UAVs can be classified into two main groups, namely, Lighter Than Air (LTA) and Heavier Than Air (HTA) as shown in Fig. 1, VTOL is one type of aerial vehicles which has the ability of vertical and stationary flight. Quadrotor UAV is one of the most famous and widely used VTOL vehicles configurations [1]. Quadrotor UAV is the target of numerous investigations within the last decade e.g. [2], [3], [5] and [6].

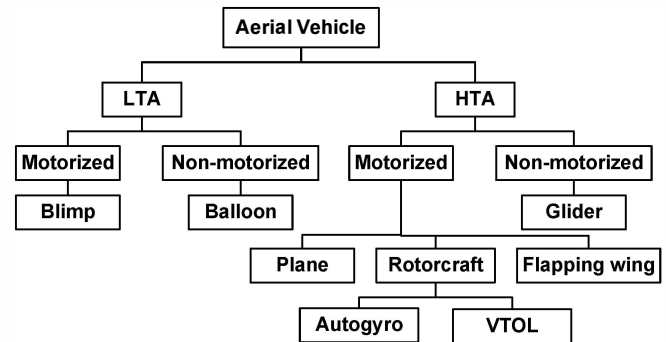


Figure 1. Aircraft classification^[1]

Quadrotor is commonly defined as a mechatronic system which has four-rotor in a cross configuration. The quadrotor is controlled based on the balance between the resultant four forces, shown in Fig. 2, in which two pairs of rotor are rotating in the opposite direction of the other pairs in order to eliminate the aerodynamic torques. Lift of the quadrotor is achieved by increasing (or decreasing) all rotor speeds by the same amount. Increasing (or decreasing) the relative speed of left and right rotors produces torque which leads to rotation around the X-axis by an angle called Roll(ϕ). Increasing (or decreasing) the relative speed of the front and rear rotors produces torque which leads to rotation around the Y-axis axis by an angle called Pitch(θ). Finally, increasing (or decreasing) the speed of the left-right rotor pair relative to the speed of the front-rear rotor pair produces torque which leads to rotation around the Z-axis by an angle called Yaw(ψ).

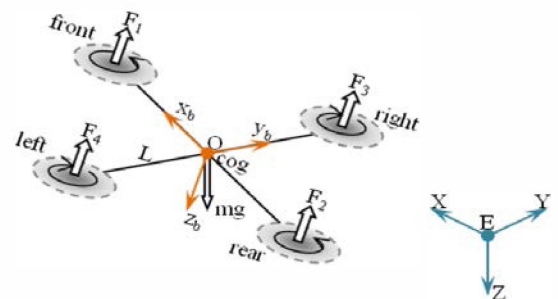


Figure 2. Principal of quadrotor control^[2]

Flexible maneuverability and simple mechanics is another advantage of utilizing the quadrotor UAV. However, the inherent Nonlinearity of the quadrotor system adds challenge against system stabilization. Many researches invested significant effort in different stabilization control algorithms such as PD and PID classical controller which succeeded to efficiently control the quadrotor system in hover condition. However, these controllers couldn't stabilize the quadrotor in presence of strong perturbations [2], [3] and [4], Linear Quadratic Regulators (LQRs) is another technique that was widely studied to minimize the tracking error by minimizing a cost function. Simulations of a quadrotor path following using LQR for various maneuver missions were conducted in [2] and [5]. Wu Y. recommended Nonlinear controller using feedback linearization as a promising technique for stabilization of quadrotor as a result of comparative study between three different control techniques namely, simple PD controller, PD controller with Partial differential, and Nonlinear feedback linearization based control [3]. The simulation results support the utilization of Nonlinear feedback control for attitude stabilization [3] and [6].

In this article, an optimized feedback linearization control algorithm is developed along with the classical PD with low pass filter controller. The parameters of each controller are optimized to set the time-domain performance within specific constrains. Simulation and real time experiments show the superiority of the optimized Nonlinear control strategy over the linear one. The Nonlinear feedback controller proves the ability to stabilize both roll and pitch angles at the same time while classical PD controller, with low pass filter, can only deal with one of these two angles at a time, as shown in the result and analysis section.

II. MATHEMATICAL MODEL OF QUADROTOR

The quadrotor system mathematical model was the focus of many researchers in the last decade such as [1], [2], [4] and [5]. Inertial frame outside the model at a fixed point and body frame with its origin located in the quadrotor center of mass were assumed to model the quadrotor system, as shown in Fig. 3

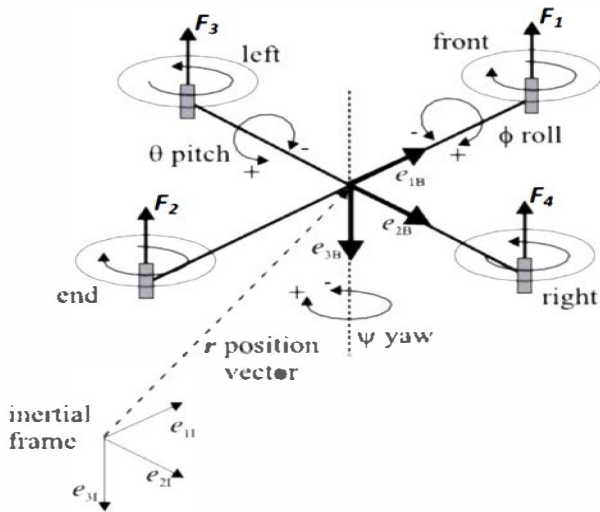


Figure 3. Configuration, inertial and body fixed frame of the quadrotor^[6]

Quadrotor orientation is defined by three Euler angles namely roll angle (ϕ), pitch angle (θ) and yaw angle (ψ). These can be represented in the vector form $\mathbf{\Omega}^T = (\phi, \theta, \psi)$. Vehicle position is defined by the vector $\mathbf{r}^T = (x, y, z)$. The body fixed frame is transformed to the inertial frame by the rotational matrix \mathbf{R} where $\cos\phi$ is denoted by c_ϕ and $\sin\phi$ is denoted by s_ϕ :

$$\mathbf{R} = \begin{pmatrix} c_\psi c_\theta c_\phi s_\phi s_\phi - s_\psi c_\phi c_\psi s_\theta c_\phi + s_\psi s_\phi \\ s_\psi c_\theta s_\psi s_\phi s_\phi + c_\psi c_\phi s_\psi s_\theta c_\phi - c_\psi s_\phi \\ -s_\theta c_\theta s_\phi c_\phi c_\phi \end{pmatrix} \quad (1)$$

The position of the quadrotor is obtained by Newton's second law of motion as:

$$m \cdot \ddot{\mathbf{r}} = m \cdot \mathbf{g} \cdot \begin{pmatrix} 0 \\ 0 \\ 1 \end{pmatrix} - \mathbf{R} \cdot \mathbf{T} \cdot \begin{pmatrix} 0 \\ 0 \\ 1 \end{pmatrix} \quad (2)$$

where \mathbf{T} is the thrust force and defined as:

$$\mathbf{T} = \sum_{i=1}^4 |F_i| = b \sum_{i=1}^4 \omega_i^2 \quad (3)$$

$i = 1:4$, b is the thrust coefficient and ω_i is the speed of the rotors.

The orientation of the quadrotor can also be obtained from

$$\mathbf{I} \ddot{\mathbf{\Omega}} = -(\dot{\mathbf{\Omega}} \times \mathbf{I} \dot{\mathbf{\Omega}}) - \mathbf{M}_R + \mathbf{M} \quad (4)$$

The applied torque is defined by:

$$\mathbf{M} = \begin{pmatrix} lb(\omega_3^2 - \omega_4^2) \\ lb(\omega_1^2 - \omega_2^2) \\ d(\omega_1^2 + \omega_2^2 - \omega_3^2 - \omega_4^2) \end{pmatrix} \quad (5)$$

where, l is the lever length, \mathbf{I} is the inertia matrix, \mathbf{M}_R is the gyroscopic torque, b is the thrust coefficient and d is the drag coefficient.

Gyroscopic torque generated due to rotor rotation is defined as:

$$\mathbf{M}_R = J_R \left(\dot{\mathbf{\Omega}} \times \begin{pmatrix} 0 \\ 0 \\ 1 \end{pmatrix} \right) \cdot (\omega_1 + \omega_2 - \omega_3 - \omega_4) \quad (6)$$

where, J_R is the rotor inertia. Let's define the four inputs variables to quadrotor as:

$$\begin{aligned} u_1 &= b(\omega_1^2 + \omega_2^2 + \omega_3^2 + \omega_4^2) \\ u_2 &= b(\omega_3^2 - \omega_4^2) \\ u_3 &= b(\omega_1^2 - \omega_2^2) \\ u_4 &= d(\omega_1^2 + \omega_2^2 - \omega_3^2 - \omega_4^2) \end{aligned} \quad (7)$$

Where u_1 denotes the applied thrust force to quadrotor, u_2 denotes the net force that leads to roll torque, u_3 denotes the net force that leads to pitch torque and u_4 denotes the net force that leads to yaw torque. The gyroscopic torques depends on the rotational velocities of the rotors, hence, it depends on the vector

$u^T = (u_1, u_2, u_3, u_4)$. Therefore, the rotor speed term in (6) can be substituted by the function $g(\mathbf{u})$ for simplifications.

$$g(\mathbf{u}) = \omega_1 + \omega_2 - \omega_3 - \omega_4 \quad (8)$$

The overall dynamic model is yielded by the evaluation of (2) and (4) as follows:

$$\begin{aligned} \ddot{x} &= -(\cos\varphi \sin\theta \cos\psi + \sin\varphi \sin\psi) \cdot \frac{u_1}{m} \\ \ddot{y} &= -(\cos\varphi \sin\theta \cos\psi - \sin\varphi \sin\psi) \cdot \frac{u_1}{m} \\ \ddot{z} &= g - (\cos\varphi \cos\theta) \cdot \frac{u_1}{m} \\ \ddot{\varphi} &= \dot{\varphi} \dot{\psi} \left(\frac{I_y - I_z}{I_x} \right) - \frac{J_R}{I_x} \dot{\theta} g(\mathbf{u}) + \frac{l}{I_x} u_2 \\ \ddot{\theta} &= \dot{\varphi} \dot{\psi} \left(\frac{I_z - I_x}{I_y} \right) + \frac{J_R}{I_y} \dot{\varphi} g(\mathbf{u}) + \frac{l}{I_y} u_3 \\ \ddot{\psi} &= \dot{\varphi} \dot{\psi} \left(\frac{I_x - I(\omega_1^2 + \omega_2^2 + \omega_3^2 + \omega_4^2)_y}{I_z} \right) + \frac{1}{I_z} u_4 \end{aligned} \quad (9)$$

The state variable of the dynamic model can be written as:

$$\dot{\mathbf{x}} = \mathbf{f}(\mathbf{x}, \mathbf{u}) \quad (10)$$

Where $\mathbf{x} \in \mathbb{R}^9$ is the vector of a state variable

$$\mathbf{x}^T = (\dot{x}, \dot{y}, \dot{z}, \varphi, \theta, \psi, \dot{\varphi}, \dot{\theta}, \dot{\psi}) \quad (11)$$

From (9) and (11) the state variable is obtained as follows:

$$\dot{\mathbf{x}} = \begin{pmatrix} -(\cos x_4 \sin x_5 \cos x_6 + \sin x_4 \sin x_6) \cdot u_1/m \\ -(\cos x_4 \sin x_5 \cos x_6 - \sin x_4 \sin x_6) \cdot u_1/m \\ g - (\cos x_4 \cos x_5) \cdot u_1/m \\ x_7 \\ x_8 \\ x_9 \\ x_8 x_9 I_1 - \frac{J_R}{I_x} x_8 g(\mathbf{u}) + \frac{l}{I_x} u_2 \\ x_7 x_9 I_2 + \frac{J_R}{I_y} x_7 g(\mathbf{u}) + \frac{l}{I_y} u_3 \\ x_7 x_8 I_3 + \frac{1}{I_z} u_4 \end{pmatrix} \quad (12)$$

Where $I_1 = (I_y - I_z)/I_x$, $I_2 = (I_z - I_x)/I_y$ and $I_3 = (I_x - I_y)/I_z$.

The dynamic model can be decomposed into two main subsets. The translation of the UAV can be described by the first subset as:

$$\begin{pmatrix} \dot{x}_1 \\ \dot{x}_2 \\ \dot{x}_3 \end{pmatrix} = \begin{pmatrix} -\cos x_4 \sin x_5 \cos x_6 - \sin x_4 \sin x_6 \\ -\cos x_4 \sin x_5 \cos x_6 + \sin x_4 \sin x_6 \\ g - (\cos x_4 \cos x_5) \end{pmatrix} \cdot \frac{u_1}{m} \quad (13)$$

And the attitude of the quadrotor can be described by the second subset,

$$\begin{pmatrix} \dot{x}_7 \\ \dot{x}_8 \\ \dot{x}_9 \end{pmatrix} = \begin{pmatrix} x_8 x_9 I_1 - \frac{J_R}{I_x} x_8 g(\mathbf{u}) + \frac{l}{I_x} u_2 \\ x_7 x_9 I_2 + \frac{J_R}{I_y} x_7 g(\mathbf{u}) + \frac{l}{I_y} u_3 \\ x_7 x_8 I_3 + \frac{1}{I_z} u_4 \end{pmatrix} \quad (14)$$

III. DESIGN OF CONTROL ALGORITHM

In order to achieve quadrotor stability, the controller must be able to compensate any disturbance and return to its initial position within a minimum time. Therefore, the quadrotor attitude represents the target of the proposed controller. As shown in the block diagram, Fig. 4, the attitude control generates the actuation signal to the inverted movement matrix that computes the PWM signals required by the rotors. The quadrotor performance was tested using attitude control based on classical PD controller and feedback linearization Nonlinear controller as shown in the following subsections.

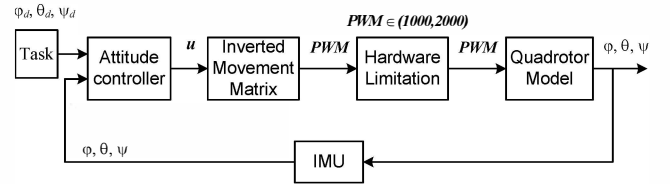


Figure 4. Attitude control block diagram

A. PD Controller

In order to simplify Equation (14), the following assumptions can be considered:

- 1) The gyroscopic term can be neglected since rotor inertias are small compared with quadrotor inertia
- 2) The Coriolis-centripetal term can also be neglected since the quadrotor can be assumed close to the hovering condition; the angular changes which come from cross coupling of angular speeds are smaller than the main.

Therefore, the simplified form of the model can be written as:

$$\begin{pmatrix} \dot{x}_7 \\ \dot{x}_8 \\ \dot{x}_9 \end{pmatrix} = \begin{pmatrix} \ddot{\varphi} \\ \ddot{\theta} \\ \ddot{\psi} \end{pmatrix} = \begin{pmatrix} \frac{l}{I_x} u_2 \\ \frac{l}{I_y} u_3 \\ \frac{1}{I_z} u_4 \end{pmatrix} \quad (15)$$

A classical PD controller has the form of,

$$u(t) = k_p e(t) + k_d \frac{de}{dt} = k_p \left(e(t) + T_d \frac{de}{dt} \right) \quad (16)$$

Usually, adding derivative action to the controller aims to improve the stability of the system. However, the derivative action has high gain for high frequency signals. This means that high frequency measurement noise will generate large variations of the control signal. In order to compensate that effect, a low pass filter of a first order with transfer function $G_f(s) = 1/(1 + T_n s)$ will be added. The PD controller with low pass

filter, as shown in Fig. 5, can be defined by three parameters k_p , $T_d = k_d/k_p$ and T_n .

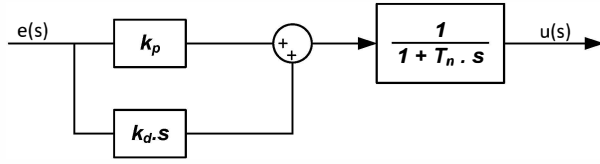


Figure 5. Block diagram of PD controller with low pass filter

B. Nonlinear control using feedback linearization

For the Nonlinear controller, the Nonlinearity due to Coriolis-centripetal term is taken into consideration. Therefore, the quadrotor model can be written as:

$$\begin{pmatrix} \dot{x}_7 \\ \dot{x}_8 \\ \dot{x}_9 \end{pmatrix} = \begin{pmatrix} x_8 x_9 I_1 + \frac{l}{I_x} u_2 \\ x_7 x_9 I_2 + \frac{l}{I_y} u_3 \\ x_7 x_8 I_3 + \frac{1}{I_z} u_4 \end{pmatrix} \quad (17)$$

New input variables u_2^* , u_3^* , u_4^* will be applied to eliminate the Nonlinearity of the plant as follows:

$$\begin{aligned} u_2 &= f_2(x_7, x_8, x_9) + u_2^* \\ u_3 &= f_3(x_7, x_8, x_9) + u_3^* \\ u_4 &= f_4(x_7, x_8, x_9) + u_4^* \end{aligned} \quad (18)$$

The following condition must be satisfied to obtain a linear system:

$$\begin{aligned} x_8 x_9 I_1 + \frac{l}{I_x} f_2(x_7, x_8, x_9) &= K_2 \cdot x_7 \\ x_7 x_9 I_2 + \frac{l}{I_y} f_3(x_7, x_8, x_9) &= K_3 \cdot x_8 \\ x_7 x_8 I_3 + \frac{1}{I_z} f_4(x_7, x_8, x_9) &= K_4 \cdot x_9 \end{aligned} \quad (19)$$

Evaluation of (19) yields the Nonlinear feedback for linearization:

$$\begin{aligned} f_2(x_7, x_8, x_9) &= \frac{I_x}{l} (K_2 \cdot x_7 - x_8 x_9 I_1) \\ f_3(x_7, x_8, x_9) &= \frac{I_y}{l} (K_3 \cdot x_8 - x_7 x_9 I_2) \\ f_4(x_7, x_8, x_9) &= I_z (K_4 \cdot x_9 - x_7 x_8 I_3) \end{aligned} \quad (20)$$

From (17), (18) and (20) the system turns into a linear system:

$$\begin{pmatrix} \dot{x}_7 \\ \dot{x}_8 \\ \dot{x}_9 \end{pmatrix} = \begin{pmatrix} K_2 \cdot x_7 + \frac{l}{I_x} u_2^* \\ K_3 \cdot x_8 + \frac{l}{I_y} u_3^* \\ K_4 \cdot x_9 + \frac{1}{I_z} u_4^* \end{pmatrix} \quad (21)$$

From (11) $\dot{x}_4 = x_7$, $\dot{x}_5 = x_8$ and $\dot{x}_6 = x_9$, than (21) can be rewritten in the form:

$$\begin{pmatrix} \ddot{x}_4 \\ \ddot{x}_5 \\ \ddot{x}_6 \end{pmatrix} = \begin{pmatrix} K_2 \dot{x}_4 + \frac{l}{I_x} u_2^* \\ K_3 \dot{x}_5 + \frac{l}{I_y} u_3^* \\ K_4 \dot{x}_6 + \frac{1}{I_z} u_4^* \end{pmatrix} \quad (22)$$

With desired angles x_{4d} , x_{5d} and x_{6d} the new inputs of the control system will be,

$$\begin{aligned} u_2^* &= w_2 (x_{4d} - x_4) \\ u_3^* &= w_3 (x_{5d} - x_5) \\ u_4^* &= w_4 (x_{6d} - x_6) \end{aligned} \quad (23)$$

Equations (22) and (23) lead to second order closed-loop systems with the transfer functions.

$$\begin{aligned} \frac{X_4(s)}{X_{4d}(s)} &= \frac{w_2}{I_x/L \cdot s^2 - K_2 I_x/L \cdot s + w_2} \\ \frac{X_5(s)}{X_{5d}(s)} &= \frac{w_3}{I_y/L \cdot s^2 - K_3 I_y/L \cdot s + w_3} \\ \frac{X_6(s)}{X_{6d}(s)} &= \frac{w_4}{I_z \cdot s^2 - K_4 I_z \cdot s + w_4} \end{aligned} \quad (24)$$

The performance of these closed-loop systems are then determined by the parameter pairs (K_2, w_2) , (K_3, w_3) and (K_4, w_4) , taking into consideration the hardware limitation.

IV. RESULTS AND ANALYSIS

The quadrotor system parameters required for simulation and running were evaluated experimentally by measuring the brushless motor thrust and drag coefficients. All the identified parameters of the quadrotor system are shown in Table I.

TABLE I. IDENTIFIED PARAMETERS OF THE QUADROTOR

Quadrotor Parameters	Value	Unit
l	0.25	m
g	9.81	m/s ²
m	0.511	kg
$I_x = I_y$	0.0011	kg.m ²
I_z	0.0022	kg.m ²
J_R	3.4×10^{-5}	kg.m ²
b	7×10^{-6}	kg.m
d	3×10^{-7}	kg.m ²

A. PD Controller with low pass filter

As discussed above, the classical PD controller with low-pass filter has three tuning parameters k_p , T_d and T_n that would be evaluated in order to achieve certain response requirements. The Simulink Design Optimization Toolbox, produced by MathWork Co., was utilized for optimal parameters values. The parameters were optimized to set the time-domain response within specific constraints taking into consideration the hardware limitations. Based on the manufacture data, the actuator input PWM signal should be within the operating range of (1000:2000). Through a set of trails, the time-domain response constraints were set to be ($T_s = 4 \text{ sec}$, $T_r = 1 \text{ sec}$,

and 20% overshoot) for roll and pitch angles, and ($T_s = 15 \text{ sec}$, $T_r = 2 \text{ sec}$ and 40% overshoot) for yaw angle, where T_s and T_r are the settling and rise times, respectively. The constraints of the time responses were restricted to give a practical accepted PWM value. The optimal parameters were found to be $k_p = 0.01$, $T_d = 1$ and $T_n = 0.01$ for roll and pitch angles. While for yaw angle the parameters were $k_p = 0.001$, $T_d = 1$ and $T_n = 0.01$. The behavior of the PD controller using the optimal parameters is illustrated in Fig. 6.

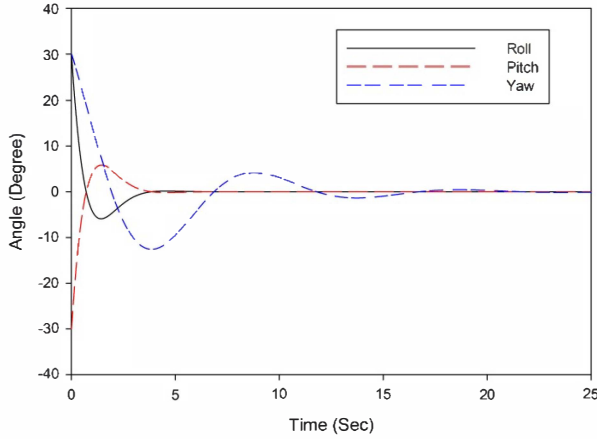


Figure 6. Simulation of PD controller response

B. Nonlinear control using feedback linearization

Nonlinear controller represents a promising solution to overcome the limitation of PD classical controller. The design parameters of Nonlinear controller are (K_2, w_2) , (K_3, w_3) and (K_4, w_4) . In contrast with the PD algorithm, it was possible to tight up the target response specifications in the optimization process based on the potentials of Nonlinear control technique. The response specifications in this case were set to be ($T_s = 4 \text{ sec}$, $T_r = 2.5 \text{ sec}$ and 1% overshoot) for roll and pitch angles, and ($T_s = 15 \text{ sec}$, $T_r = 4.5 \text{ sec}$ and 1% overshoot for yaw angle).

Using Simulink software and optimization toolbox, the optimal value of the Nonlinear controller parameters were found to be $K_2 = -2$, $w_2 = 0.0055$, $K_3 = -2w_3 = 0.0055$, $K_4 = -1$ and $w_4 = 0.0008$. The control system using the optimal Nonlinear feedback controller almost removes the overshoot of the system, as shown in Fig. 7.

The experimental testing system used for validating the developed controllers is shown in Fig. 8. First, the quadrotor was given an initial single disturbance in the three angles, one at a time. Fig. 9 through Fig. 14 shows the quadrotor responses with the optimal PD and Nonlinear controllers. The behavior comparison between the two controllers clearly indicates that Nonlinear controller has better capability to compensate the disturbance in the three Euler angles namely roll, pitch and yaw with, almost, no overshoot. However, the settling time of both PD and Nonlinear controller appears to be close to each other. The quadrotor was then given random disturbances applied repeatedly in each angle separately. Fig. 15 to Fig. 17 show the experimental responses with PD algorithm as a controller while Fig. 18 to Fig. 20 show the responses with the Nonlinear

controller. The dotted vertical lines specify the time at which disturbance are applied to the quadrotor system. It is clearly shown that both PD and Nonlinear controller can compensate the repeated random disturbance. It is important to state that this test only deals with the disturbance in only one angle at a time. In practical application, it is very difficult to guarantee that the disturbance affect only one direction. In order to validate the controller behavior under more practical conditions, a set of random disturbances were applied to the quadrotor system in the three angles simultaneously.

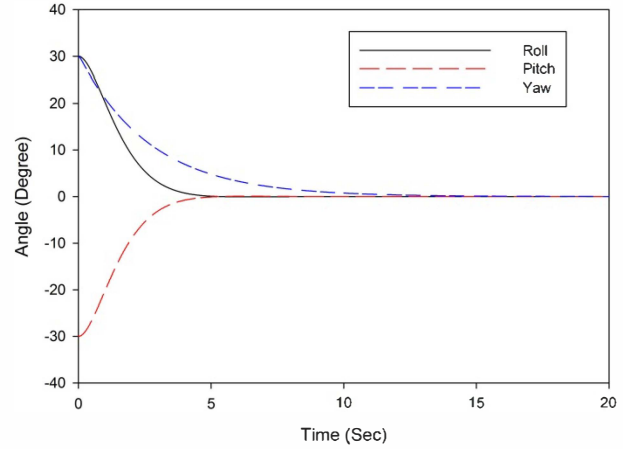


Figure 7. Simulation of Nonlinear controller using feedback linearization response

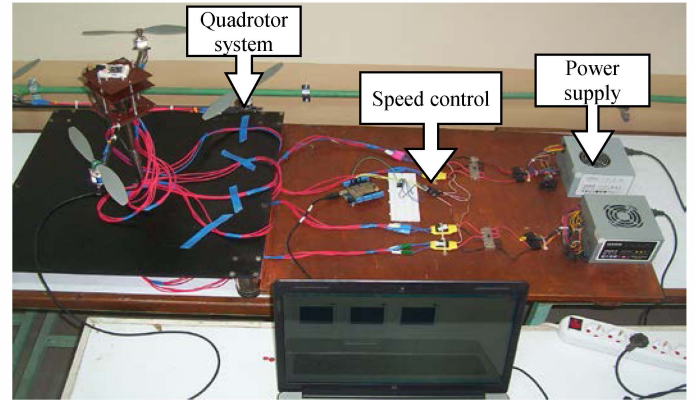


Figure 8. Quadrotor test rig

The responses of the system with the two controllers are shown in Fig. 21 for the PD controller and Fig. 22 for Nonlinear controller. As shown in the graphs, the PD controller could not compensate the quadrotor and system goes to the maximum experimental freedom limits. On the other hand, the Nonlinear controller using feedback linearization successfully reimburse the disturbance within about 5 sec maximum.

Based on the fact that practical disturbance is random and could be in more than one direction in the same time, the Nonlinear controller proves robust capability for the stabilization of the quadrotor system in comparison to classical PD controller with low pass filter. That failure of classical PD controller with low pass filter is a direct result of the interaction between the four motors which increase the Nonlinearity dynamics of the system.

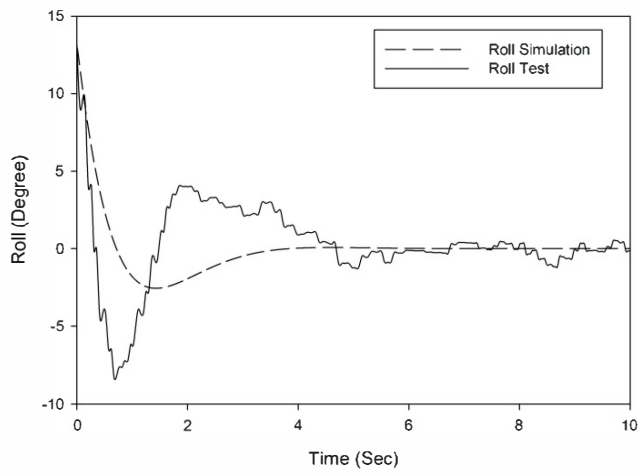


Figure 9. The PD controller behavior validation for Roll (ϕ) disturbance.

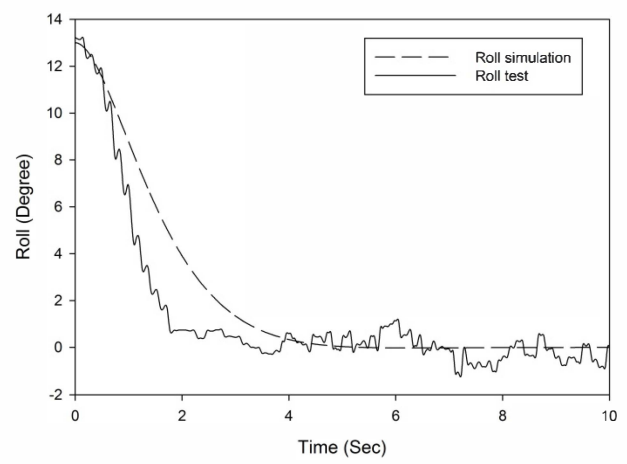


Figure 12. The Nonlinear controller behavior validation of Roll (ϕ) disturbance.

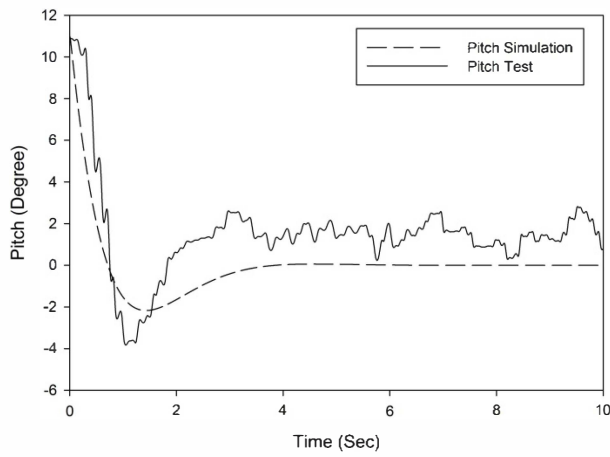


Figure 10. The PD controller behavior validation for Pitch (θ) disturbance.

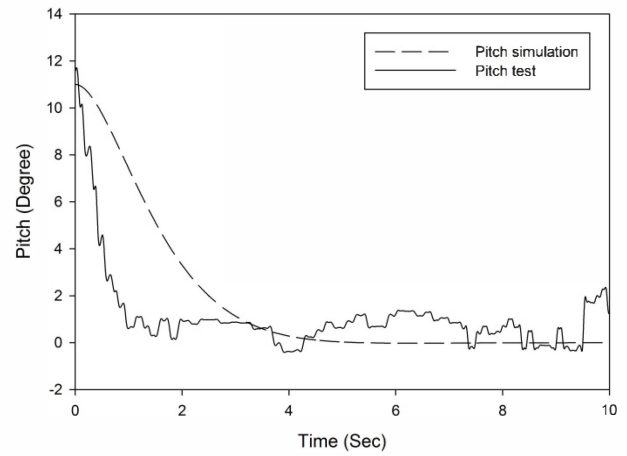


Figure 13. The Nonlinear controller behavior validation of Pitch (θ) disturbance.

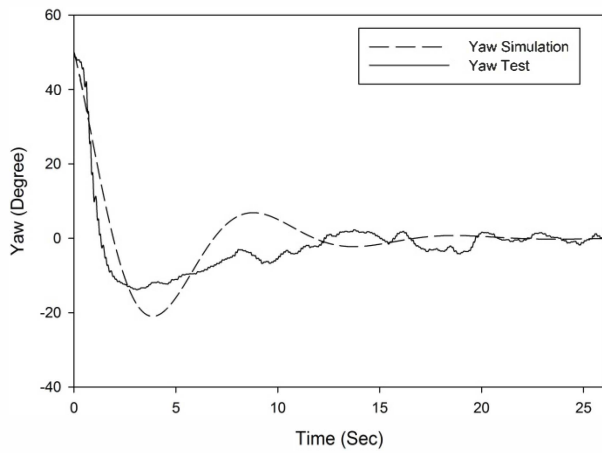


Figure 11. The PD controller behavior validation for Yaw (ψ) disturbance

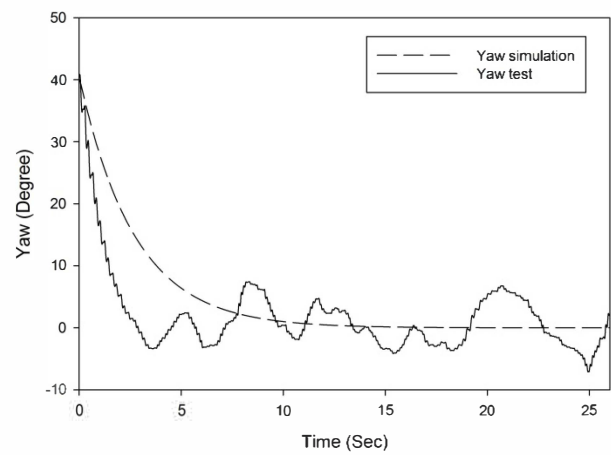


Figure 14. The Nonlinear controller behavior validation of Yaw (ψ) disturbance.

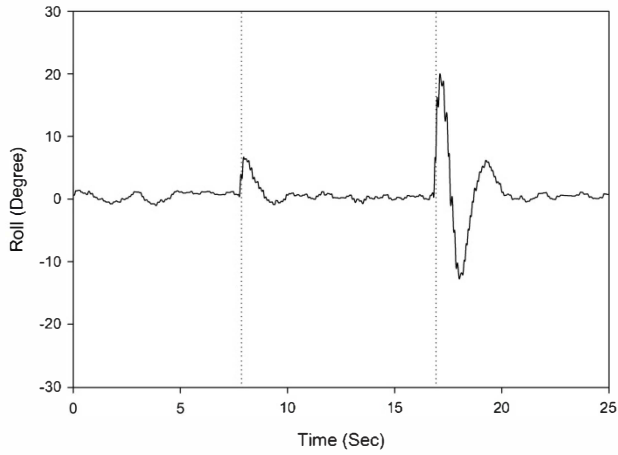


Figure 15. Response test of PD controller of Roll (φ)

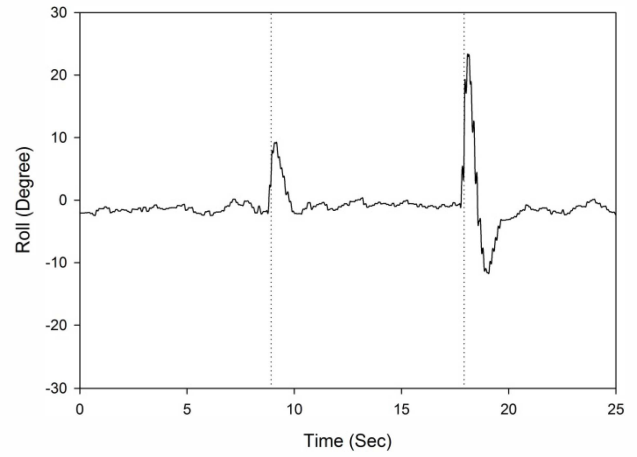


Figure 18. Response test of Nonlinear controller using feedback linearization of Roll (φ)

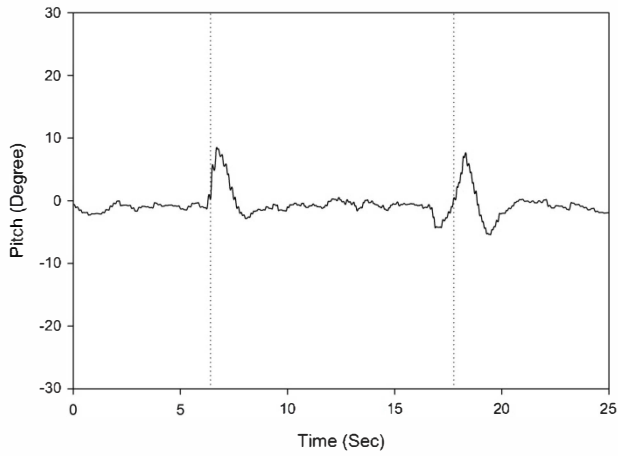


Figure 16. Response test of PD controller of Pitch (θ)

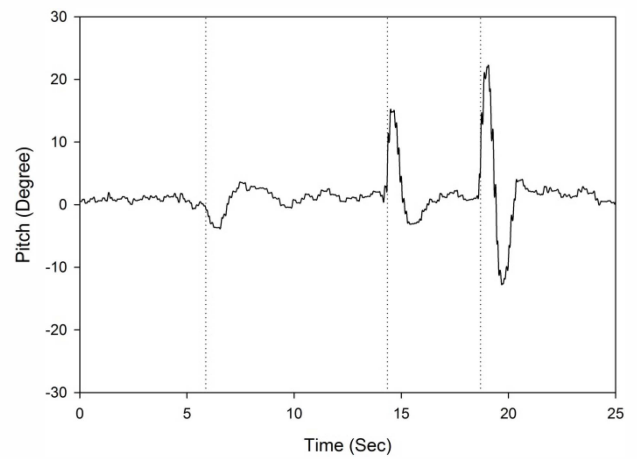


Figure 19. Response test of Nonlinear controller using feedback linearization of Pitch (θ)

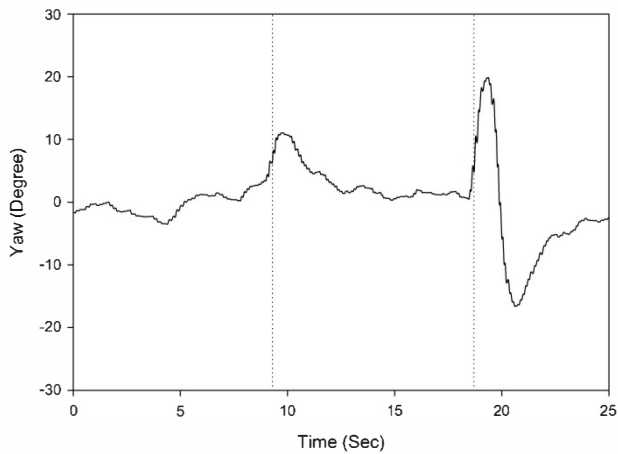


Figure 17. Response test of PD controller of Yaw (ψ)

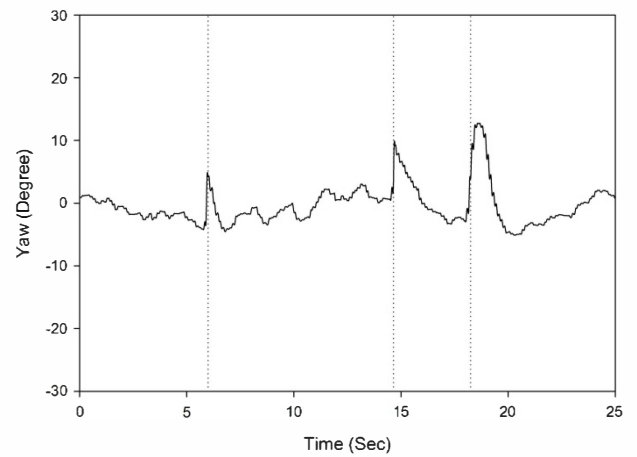


Figure 20. Response test of Nonlinear controller using feedback linearization of Yaw (ψ)

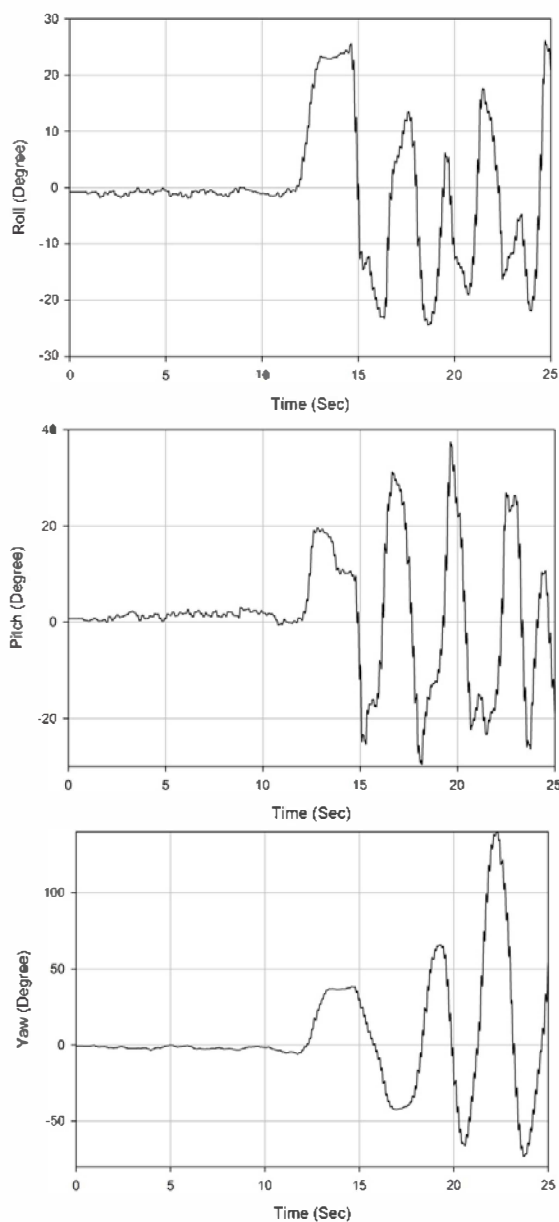


Figure 21. PD controller results of synchronously controlled Roll, Pitch and Yaw.

V. CONCLUSIONS

The results of both simulation and experimental validation tests of PD controller with low pass filter and Nonlinear controller using feedback linearization indicate the superior performance of Nonlinear controller using feedback linearization. PD controller can only deal with disturbances in only one of the Euler angles at a time since the nonlinear terms in the quadrotor model vanishes. It could not stabilize the system in case of multi angle disturbances. However, the Nonlinear controller with feedback linearization successfully stabilizes the quadrotor system with synchronous disturbances in the three Euler angles with about 5 sec to its original position. In addition, the evaluated optimal control parameters minimize the overshoot to a maximum of 1% and reduce the settling time. A real time flight test of the developed Nonlinear control with

wireless ground monitoring station is recommended in future development of this project.

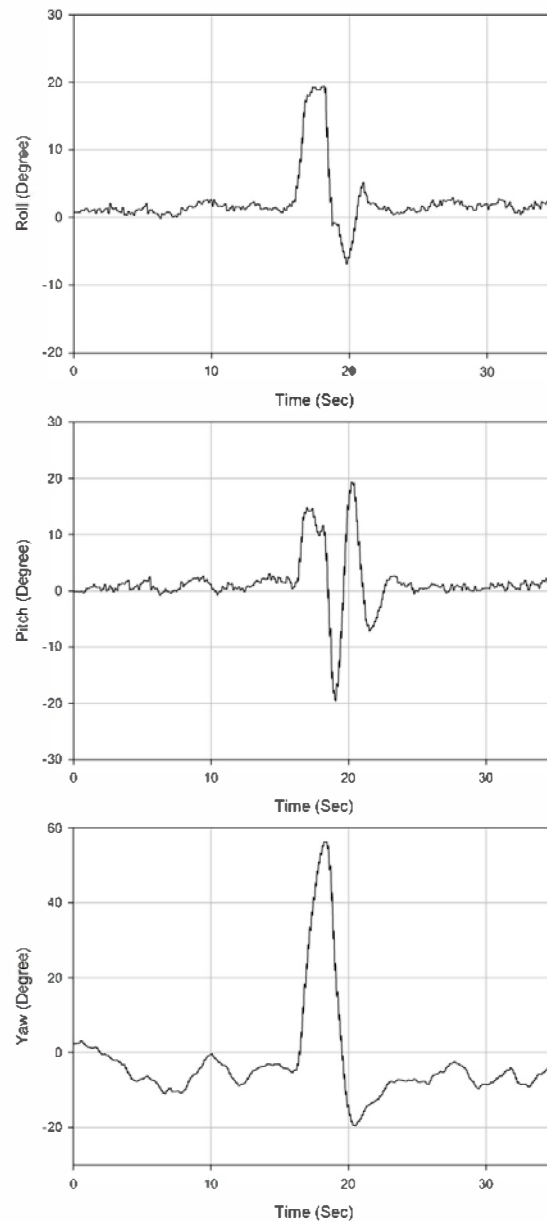


Figure 22. Nonlinear controller using feedback linearization results of Roll, Pitch and Yaw are controlled synchronously

REFERENCES

- [1] Pipatpaibul, P.-I., "Quadrotor UAV control: online learning approach", 2011.
- [2] Güçlü, A. and K.B. Arıkan, "Attitude and Altitude Control of an Outdoor Quadrotor", 2012.
- [3] Wu, Y., "Development and Implementation of a Control System for a Quadrotor UAV", Hochschule Ravensburg-Weingarten, Múptıos, 2009.
- [4] Salih, A.L., et al., "Flight PID controller design for a UAV quadrotor", Scientific Research and Essays, vol 5(23): pp. 3660-3667, 2010.
- [5] Bouabdallah, S., "Design and control of quadrotors with application to autonomous flying", Ecole Polytechnique Federale de Lausanne, 2007.
- [6] Voos, H., "Nonlinear control of a quadrotor micro-UAV using feedback-linearization", ICM 2009, IEEE International Conference on Mechatronics, 2009, pp. 1-6: IEEE.